Peer-reviewed version available at Medicina 2019, 55, 30; doi:10.3390/medicina55020030

Type of the Paper (Article)

Cell Cycle Arrest and Cytotoxic Effects of SAHA and RG7388 Mediated through $p21^{WAF1/CIP1}$ and $p27^{KIP1}$ in Cancer Cells

Umamaheswari Natarajan[1,2], Thiagarajan Venkatesan[2], Vijayaraghavan Radhakrishnan[1], Shila Samuel[1] and Appu Rathinavelu[2,3*]

[1] VRR Institute of Biomedical Science, Kattupakkam, Chennai, TN 600056, India; ubaruthrarini@gmail.com (U.N.); drrvijayaraghavan@gmail.com (V.R.); vrribms@gmail.com (S.S.)
[2] Rumbaugh-Goodwin Institute for Cancer Research, Nova Southeastern University, Ft. Lauderdale, FL 33314, USA; tvenkatesan@nova.edu (T.V.);
[3] College of Pharmacy, Health Professions Division, Nova Southeastern University, Ft. Lauderdale, FL 33314, USA
* Correspondence: appu@nova.edu; Tel.: +1-954-262-0411; Fax: +1-954-262-3825

Abstract: Alterations in gene expressions are often due to epigenetic modifications that can lead to significant influence on cancer development, growth, and progression. The main epigenetic modifications observed in human are methylation and acetylation. In this regard, the HDAC inhibitors (HDACi) such as SAHA (Vorinostat), which can exert epigenetic alterations through impacting the acetylation status of histones, are in clinical trials as a new class of drugs with promising effects on the cancer growth and metastatic process. The small molecule RG7388 is a newly developed inhibitor that is specific for an oncogene-derived protein called MDM2, which is in clinical trials for the treatment of various types of cancers. One of the common characteristics for these two drugs is their ability to induce p21 expression through distinct mechanisms in MCF-7 and LNCaP cells. This difference was expected trigger cell cycle arrest and cell death through intra-cellular mechanisms that are not identical. Hence, the molecular mechanism whereby SAHA can induce cell cycle arrest and trigger necrosis, apoptosis or necroptosis is still evolving. Similarly, the ability of RG7388 for producing anticancer effect is undergoing thorough investigation, since it can produce p53 dependent and p53 independent effects. In this study we performed experiments to measure the cell cycle arrest effects of SAHA and RG7388 on using MCF-7 and LNCaP cells. The cytotoxicity, cell cycle arrest and apoptosis / necroptosis effects of the treatments were assessed by using Trypan Blue Dye Exclusion (TBDE) method, MTT assay, Fluorescence assay with DEVD-*amc* fluorogenic substrate and Immunoblotting methods. Our results from MCF-7 and LNCaP cells confirmed that SAHA and RG7388 treatments were able to induce cell death via combination of cell cycle arrest and cytotoxic mechanisms. We are speculating that our findings could lead to the development of newer treatments for breast and prostate cancers using this type of combinations.

Keywords: SAHA; RG7388; MDM2; p53; p21; Cell Cycle Arrest; Cell Death

Peer-reviewed version available at Medicina 2019, 55, 30; doi:10.3390/medicina55020030

1. Introduction

Breast cancer is one of the most common causes of cancer-related deaths worldwide. Despite the continued efforts around the globe, there has been only marginal improvements in breast-cancer-related treatment success. The median survival time for patients with metastatic breast cancer is no more than 1 year [1]. The survival rate for prostate cancer patients with distant metastasis is only around 30% versus the 99% survival rate for patients with localized disease. Therefore, the need for new drugs and efficient strategies for effectively treating aggressive cancers continues to exist. Although the development of cancer is triggered by a complex process of tumorigenesis, they are intimately linked to gene mutations and abnormal gene expressions. Therefore, epigenetic changes, which are known to affect the gene transcription without modifying the underlying DNA sequence, are also very common and significant in the process of tumorigenesis. In normal cells the histones are modified via acetylation, methylation and phosphorylation to meet certain needs of the cellular function [2,3]. Acetylation of histone is one of the most common epigenetic modifications that is regulated largely by histone acetyltransferases (HATs), which transfer the hydrophobic acetyl group from acetyl coenzyme A to specific lysine residues on the N-terminal tails of histone H2A, H2B, H3 and H4 [4].

The addition of acetyl groups to histones lead to the neutralization of positive charges of the amino groups and increases the steric interference that can loosen the histone-DNA structure and makes it more accessible for transcription machinery. On the other hand, the DNA stretching and activation of the gene expression can be turned off when histone is deacetylated [5,6]. The histone deacetylation is carried out by enzymes that belong to two families, the classical HDAC family and SIR2 family [7]. Totally there are 11 HDAC isoenzymes that deacetylate histones within the nucleus, and the specific HDACs are differentially regulated to modulate the expression of various groups of genes [8]. When histone deacetylase inhibitor such as SAHA is used, the gene expression can be activated. Enhanced expressions of tumor suppressors and checkpoint inhibitors such as $p21^{WAF1/CIP1}$ and $p27^{KIP1}$ that can lead to suppression of cell differentiation, growth arrest, apoptosis, and autophagy indicating that the net effect of histone acetylation blockade is inhibition of cell proliferation [9,10,11]. Hence, several HDACi, including SAHA (Suberoylanilide Hydroxamic Acid also known as Vorinostat), have been reported to stimulate much enthusiasm in the field of oncology with more than 40 clinical trials initiated to date.

Another gene that is important in the cell cycle regulation, tumor growth and angiogenesis is MDM2 [12]. In several metastatic sarcomas MDM2 gene has been shown to encode a protein in the molecular weight range of 90 KD (p90), that can form an oligomeric complex with both mutant and wild type p53 proteins. The interaction between MDM2 and p53 is believed to occur through direct binding by involving a specific binding domain on the MDM2 protein [13,14,15]. In addition, it has been well established that MDM2 contains an ubiquitin ligase (E3) activity in its carboxy terminus which is responsible for the poly-ubiquitination of p53 and consequent proteasomal degradation [16]. Initially it was believed that only the full length MDM2 protein (p90) could act as a negative regulator in cells that contain genetically intact p53 gene and abolish cell cycle control mechanisms. However, studies on MDM2 splice variants, including the ones lacking p53 binding domains, have suggested that mechanisms other than p53 suppression could also be involved in promoting malignancy during MDM2 gene amplification [17,18]. So far, more than 40 alternatively spliced variants of MDM2 gene transcripts have been identified in various tumor cells, but it is unknown at this time whether all of

the splice variants are translated into protein. In fact, some of the splice variants have been detected only in a few particular tumor types suggesting that, these splice variants might even contribute to the phenotype transformation of tumor cells, whereas others such as MDM2-A and MDM2-B may be associated with tumorigenesis in general [19]. So far, our preliminary studies have clearly suggested that MDM2 protein may be critically involved in the transcription control of VEGF expression in several cancers and promote tumor angiogenesis [20,21].

`One of the effective methods of blocking MDM2 mediated mechanisms is by inhibiting its interaction with p53 protein. Historically, disruption of protein-protein interaction used to be a challenging task due to the large binding interface of the protein partners. However, the small interface of MDM2-p53 made it possible to design small-molecule inhibitors such as RG7388 to target the MDM2-p53 interaction. Although very little progress was made in the initial few years after deriving the crystal structure of the MDM2-p53 complex, lately several classes of small-molecule inhibitors with distinct chemical structures and properties have been reported. An actual breakthrough in the design of the small-molecule inhibitors for MDM2 was achieved through the discovery of Nutlin by Vassilev and colleagues [22]. However, many of the initially designed molecules were not utilized in clinical trials because of limited *in vivo* potency, poor bioavailability and excessive toxicity [23]. By keeping the initial setback in mind, a new generation of MDM2 inhibitors were developed to optimize potency and bioavailability. In this regard, the RG7388 small molecule, belongs to the new generation of MDM2 inhibitors with good selectivity and improved bioavailability [24]. Several studies that were conducted by utilizing RG7388, to effectively rescue p53 and activate downstream apoptotic pathways in p53 wild-type cell lines, so far have yielded interesting results [25]. However, the detailed mechanisms of cell cycle arrest and cell death induced by HDAC inhibitor SAHA and MDM2 inhibitor RG7388 has not been fully established. Moreover, the HDACi function of SAHA is not only limited to modifying the acetylation status of histones but also is suspected to be involved with the modification of non-histone proteins including p53. Therefore, a possible interaction or synergy between HDACi and MDM2 inhibitors were speculated. The current study has provided some interesting insights into the mechanisms mediated by these two inhibitors, which strongly impact p21 expression.

2. Materials and Methods

2.1. Reagents

Histone deacetylase (HDAC) inhibitor SAHA was purchased from Selleckchem (Houston, TX, USA) and MDM2 inhibitor RG7388 was purchased from MedChemExpress (New Jersey, MCE, USA). ECL was purchased from KPL biosolutions (Milford, MA). The primary antibodies against p53, p21, p27, AURKB, CDC25C, CDK1, BAK, BAX and Cleaved PARP (1:1000) were purchased from Cell Signaling Technology, (Danvers, MA, USA). MDM2 antibody (1:500) Mouse monoclonal) was purchased from Santa Cruz biotechnology. β-actin (1:2000) was purchased from Sigma Aldrich chemical company (St. Louis, MO, USA). The secondary antibodies anti-rabbit, anti-mouse, and HRP conjugated and DMSO were purchased from Sigma Aldrich chemical company (St. Louis, MO, USA). Nitrocellulose membrane (0.45 μm) was purchased from Amersham (GE Healthcare Life Sciences USA). ECL was purchased from KPL biosolutions (Milford, MA). DEVD-*amc* CellEvent™ Caspase-3/7 Green ReadyProbe™ was purchased from Thermo Fisher (Molecular Probes, Life Technologies, USA). All other chemicals used in this experiment were of research grade.

2.2. Cell Culture and Drugs Treatment

Human breast adenocarcinoma cell line (MCF-7) was obtained from American Type Culture Collection (Manassas, VA, USA). Human prostate adenocarcinoma cell line (LNCaP) was provided by Dr. Thomas Powell (Cleveland Clinic Foundation, Cleveland, OH). The MCF-7 cells and LNCaP were cultured with Dulbecco's Modified Eagle's Medium (DMEM) and RPMI-1640, supplemented with 10% fetal bovine serum (FBS), 1% L-glutamine, 1.5 g/L sodium bicarbonate antibodies (1% Amphotericin B and 1% penicillin G - Streptomycin). The cells were maintained in a humidified atmosphere with 95% air and 5% CO_2 at 37°C. When MCF-7 and LNCaP cells reached 75-80% confluency, we were treated with 7.5 μM of SAHA, 2.0 μM of RG7388 for 24 hrs. After incubation the cells were used for protein extraction, for western blot analysis. Similarly, the cell viability assays and Fluorescence staining were also performed after treating the cells with the above mentioned scheme.

2.3. Cell viability assessment using MTT and Trypan Blue Dye Exclusion Method

The MCF-7 and LNCaP cells were plated at a density of $5x10^3$cells/well in 96-well plates, and incubated at 37°C under 95% air and 5% CO_2 for 24 hrs. Once the cells reached 75-80% confluency they were treated with different concentrations of the drugs for 24 hrs. After incubation, the viability of the cells were assessed using Trypan Blue Dye Exclusion method (TBDE) and 3-(4,5-dimethylthiazol-2-yl)-2,5-diphenyltetrazolium bromide (MTT) assay. In the TBDE method, after removing the incubation medium, equal parts of 0.4% trypan blue dye to the cell suspension was added. The mixture was allowed to incubate for less than three minutes at room temperature. The cell viability was counted using the TC20 automated cell counter from Bio-Rad (Hercules, CA). In MTT assay, the cells were seeded into a 96-well plate at a density of 5×10^3 per well (200 μl) and treated with the following: control and SAHA (0.5, 2.5, 5.0, 7.5, and 10.0 μM) and RG7388 (1.0, 2.0, 2.5, 5.0, and 7.5 μM). After 24 hrs of treatment, 20 μl of MTT solution (5 mg/ml in PBS) was added to each well and the cells were incubated at 37°C for an additional 3-4 hrs. At the end of incubation, 200 μl of DMSO was added to each well. The plate was gently rotated on an orbital shaker for few minutes to completely dissolve the precipitates. The absorbance was read at 650 nm with a Versamax microplate reader (Molecular Devices, Sunnyvale, CA, USA).

2.4. Protein Preparation and Western Blot Analysis

After 24 hrs of treatment the cells were lysed with RIPA (Radio-Immunoprecipitation Assay) buffer, containing the protease inhibitor cocktail and sodium orthovanadate (Santa Cruz Inc., Dallas, TX, USA), for 30 min at 4°C. Cell lysates were clarified by centrifugation at 4°C for 20 min at 14,000 rpm. The concentrations of proteins in the clarified samples were determined by using bicinchoninic acid (BCA) protein assay method (Thermo Fisher Scientific, Grand Island, NY, USA). For the western blot analysis equal concentration of proteins were separated using 7.5-12% sodium dodecyl sulfate-polyacrylamide gel electrophoresis (SDS-PAGE) and blotted onto a nitrocellulose membrane. After transfer of proteins, the membranes were blocked using 5% non-fat dry milk and then probed with specific antibodies including MDM2, p53, p21, $p27^{Kip1}$, Aurora Kinase-B, CDC25C, CDK1, BAK, BAX, Cleaved PARP and β-actin. Finally, detection of specific protein bands on the membranes was achieved by incubating in a solution containing LumiGLO Reserve Chemiluminescent substrate

(KPL, Gaithersburg, MA, USA). Densitometric analyses were performed using the ImageJ program (NIH Image, Bethesda, MD).

2.5. Fluorescence Imaging for Cell Death Assessment

The fluorescent caspase substrate DEVD-*amc* is a cell permeant Caspase-3/7 substrate that consists of a four-amino acid peptide (DEVD) conjugated to a nucleic acid-binding dye *amc* (7-Amino-4-methylcoumarin). The peptide sequence is based on the PARP cleavage site Asp^{216} for Caspase-3/7. Uncleaved DEVD-*amc* is intrinsically non-fluorescent, when it was not bound by the DNA. During apoptosis, caspase-3 and caspase-7 proteins are activated the conjugate is cleaved so that free dye can stay intracellular and bind to DNA. Thus, cleavage of the Caspase-3/7 recognition sequence label the apoptotic cells, generating a bright green fluorescence. Once cleaved from DEVD the *amc* that is binding to DNA can be excited at 502 nm to emit fluorescence that can be measured at 535 nm. For determining the effects of the drugs, the cells were treated with SAHA, RG7388 for 24 hrs. After the drug treatment the cells were washed and then incubated with the Caspase-3/7 Green DEVD-*amc* substrate for 15-30 minutes. The fluorescence in the apoptotic cells was measured using Victor 3 Spectrofluorometer.

2.6. Statistical Analysis

The data are presented as mean ± SD from Statistical significance between the groups was analyzed by one-way analysis of variance (ANOVA) followed by LSD (Least Significant Difference) test. $P < 0.05$ was considered statistically significant.

3. Results

3.1. Reduction level of Cell viability by SAHA and RG7388 treatments on MCF-7 and LNCaP cells

Arresting cell cycle and inducing apoptosis is one of the primary goals of cancer treatments. In this regard, our studies were designed to specifically analyze the intracellular events following SAHA and RG7388 treatments using MCF-7 and LNCaP cells. During the cell viability assessment experiments, both the Trypan Blue Dye Exclusion (TBDE) and MTT assay methods were employed. The treatment effects of SAHA are shown in (Figures 1A-2A). Following treatments both SAHA and RG7388 produced significant reduction in the cell viability after 24 hrs, as we can be seen in (Figure 1B-2B). The IC_{50} for SAHA after 24 hrs of treatment was found to be 7.5 μM. On the other, RG7388 produced stronger cytotoxic effects on LNCaP cells and therefore the IC_{50} was found to be 2.0 μM after 24 hrs of treatment (Figure 2A-2B). In MCF-7 cells also SAHA and RG7388 treatments produced similar IC_{50} values (Figure 1A-1B).

201

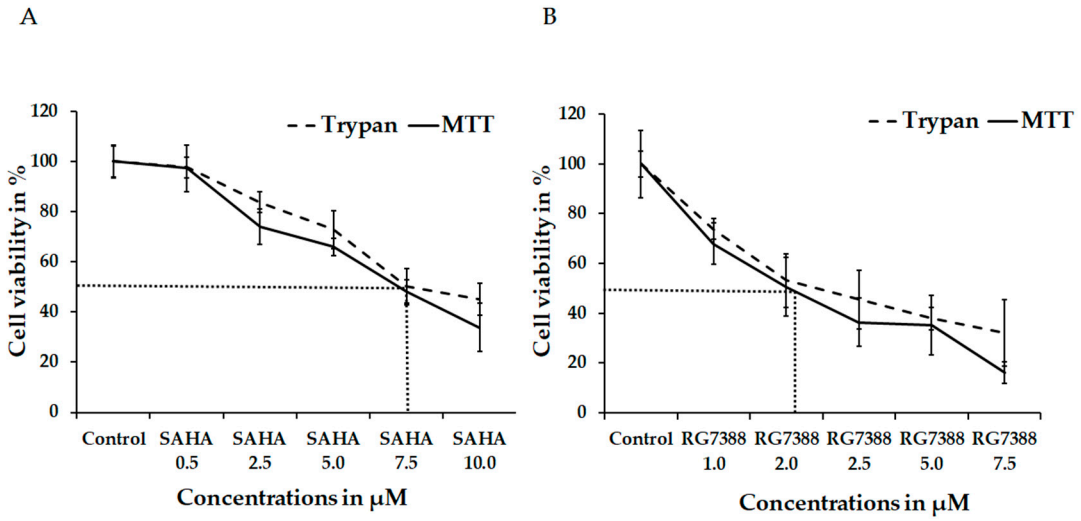

202 **Figure 1.** Assessment of Cell Viability using Trypan Blue Dye and MTT on MCF-7 Cells after treating
203 with SAHA and RG7388. The effect of 24 hrs treatment on MCF-7 cell viability was assessed using
204 0.5, 2.5, 5.0, 7.5, 10.0 µM concentrations of SAHA (A), and 1.0, 2.0, 2.5, 5.0, 7.5 µM concentration of
205 RG7388 (B). The data are presented as means ± S.E.M. from minimum of three independent
206 experiments.

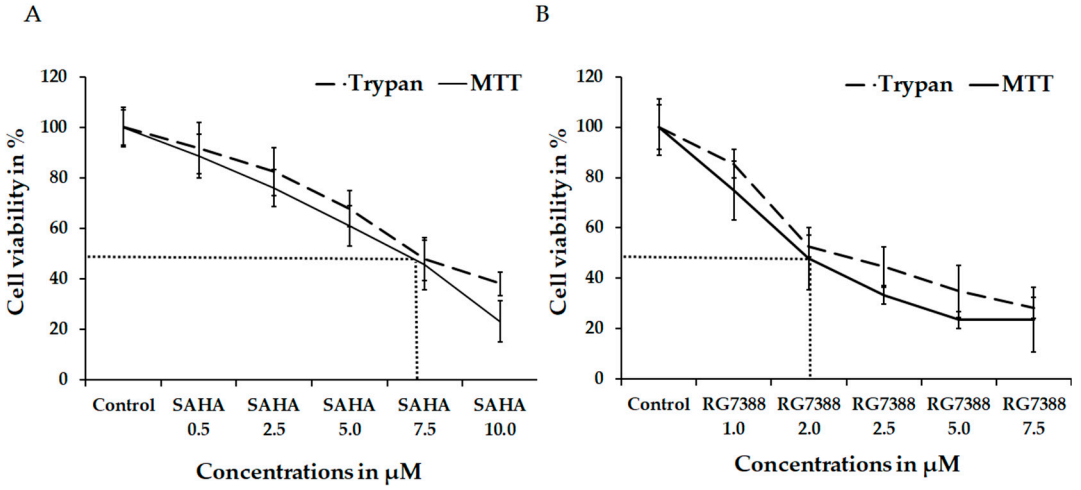

207 **Figure 2.** Assessment of Cell Viability using Trypan Blue Dye and MTT on LNCaP Cells after treating
208 with SAHA and RG7388. The effect of 24 hrs treatment on LNCaP cell viability was assessed using
209 0.5, 2.5, 5.0, 7.5, 10.0 µM concentrations of SAHA (A), and 1.0, 2.0, 2.5, 5.0, 7.5 µM concentration of
210 RG7388 (B). The data are presented as means ± S.E.M. from minimum of three independent
211 experiments.
212

3.2. Effect of SAHA and RG7388 treatments on $p21^{WAF1/CIP1}$ and $p27^{Kip1}$ Levels

Based on the results shown in Figure 4, both SAHA and RG7388 induced strong cell cycle arrest in LNCaP cells. In addition, treatments with SAHA and RG7388 showed elevation in the levels of $p21^{WAF1/CIP1}$. The elevation caused by SAHA was only around 1.3 folds whereas RG7388 treatment induced 3.5 folds increase in $p21^{WAF1/CIP1}$ levels. However, treatment of LNCaP cells with SAHA did not elevate neither MDM2 nor p53 protein levels after 24 hrs of treatment. As expected RG7388 treatment elevated both MDM2 and p53 levels by nearly 95% and 120% respectively in the LNCaP cells (Figure 4). The results observed with MCF-7 were quite interesting because, only SAHA treatment was able to increase $p21^{WAF1/CIP1}$ levels whereas RG7388 treatment did not increase the levels of $p21^{WAF1/CIP1}$. On the contrary, RG7388 was able to significantly elevate the levels of p53 in MCF-7 cells while SAHA treatment did not alter the levels of p53 (Figure 3). In addition to the $p21^{WAF1/CIP1}$ levels, the results of the $p27^{Kip1}$ levels following SAHA treatment suggested an interesting mechanism in both cell lines. The $p27^{Kip1}$ levels were significantly elevated by nearly 300% in both LNCaP and MCF-7 cells after 24 hrs of treatment. Though RG7388 treatment elevated $p27^{Kip1}$ levels in LNCaP and MCF-7 cell lines, the increase was lower than what was seen with SAHA treatment and, it was only around 90% in these cell lines. It is interesting that in LNCaP cells SAHA was able to induce $p21^{WAF1/CIP1}$ expression without any significant changes in the expression levels of p53. Thus, our results clearly suggested that, SAHA treatment can significantly elevate $p21^{WAF1/CIP1}$ and $p27^{Kip1}$ expressions in both cell lines, while RG7388 treatment was able to markedly elevate $p21^{WAF1/CIP1}$ along with only slight elevation of $p27^{Kip1}$ expression in LNCaP cells. Such elevation following RG7388 treatment was completely absent in MCF-7 cells.

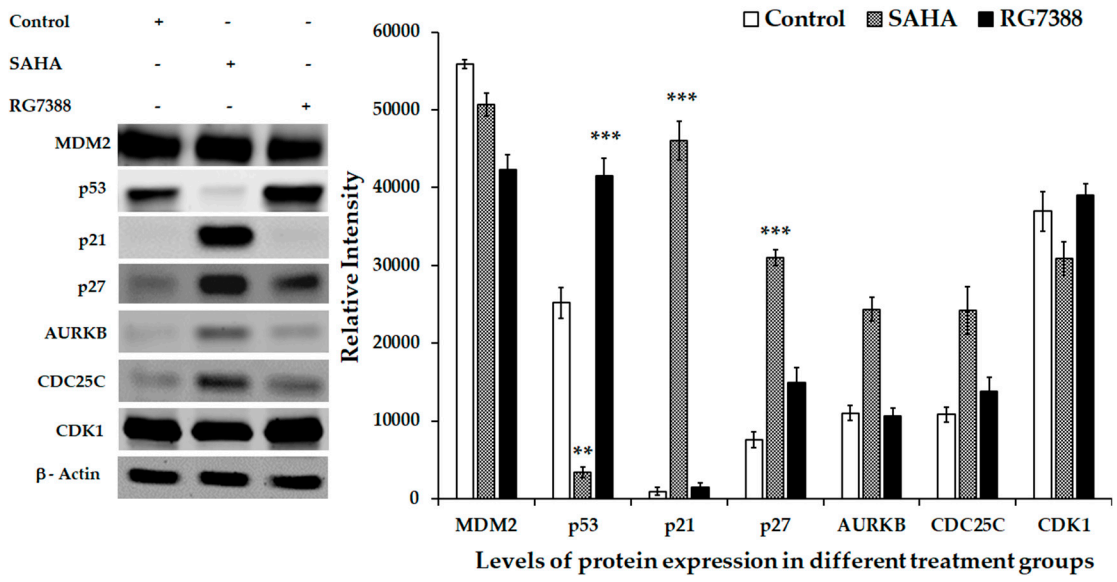

Figure 3. Effect of SAHA and RG7388 treatments on Cell Cycle related Protein levels in MCF-7 cells. Figure shows upregulation of p21, p27, AURKB and CDC25C levels after treatment with 7.5 μM concentration of SAHA and p53 upregulation after RG7388 treatment. Downregulation of MDM2 and p21 level in cells after treatment with RG7388. The right panel shows the results of relative band intensity of the western blots bands that were measure using ImageJ software. The normalization of

Preprints (www.preprints.org) | NOT PEER-REVIEWED | Posted: 7 October 2018 doi:10.20944/preprints201810.0121.v1

Peer-reviewed version available at Medicina 2019, 55, 30; doi:10.3390/medicina55020030

protein levels are depicted using the band intensities of β-actin bands. Data are presented as means ± S.E.M. from minimum of three independent experiments. *, P < 0.05 vs. Control; **, P < 0.001 vs. Control; ***, P < 0.01 vs. Control.

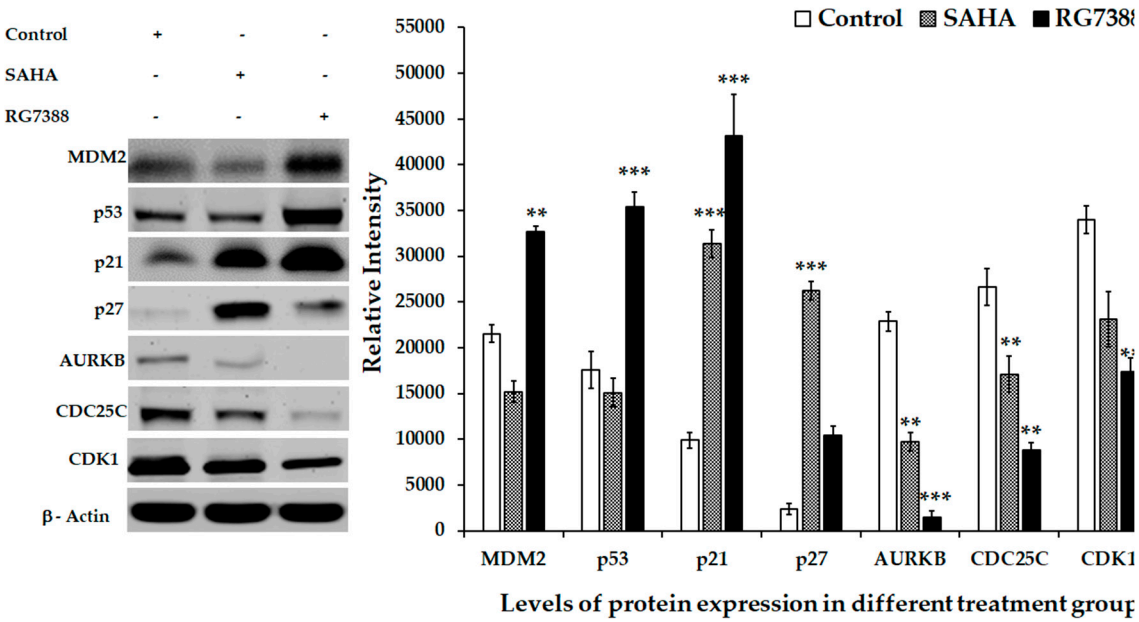

Figure 4. Effect of SAHA and RG7388 treatments on Cell Cycle related Protein levels in LNCaP cells. Figure shows upregulation of p53, p21 and MDM2 levels after treatment with 2.0 μM concentration of RG7388 and p21, p27 upregulation after treatment with 7.5 μM concentration of SAHA. Downregulation of AURKB, CDC25C and CDK1 levels after treatment with SAHA and RG7388. The right panel shows the results of relative band intensity of the western blots bands that was measure using ImageJ software. The normalization of protein levels are depicted using the band intensities of β-actin bands. Data are presented as means ± S.E.M. from minimum of three independent experiments. *, P < 0.05 vs. Control; **, P < 0.001 vs. Control; ***, P < 0.01 vs. Control.

3.3. Aurora kinase-B (AURKB), CDC25C and CDK1 levels in SAHA and RG7388 Treated Cells

In addition to the expression results of CDKI (Cyclin Dependent Kinase inhibitors) that are discussed in the previous section, a significant decrease in AURKB, CDC25C and CDK1 were also noted in LNCaP cells, following both SAHA and RG7388 treatments (Figure 4). However, the changes in the levels of the above mentioned cell cycle regulators were marginal with RG7388 treatment in MCF-7 cells while SAHA treatment showed noticeable elevation of AURKB and CDC25C levels (Figure 3). This observation suggested that the mechanism of cell cycle arrest and cell death in these two cell lines are distinct with sufficient cross-talk between the cell cycle and apoptosis pathways involved.

3.4. Apoptotic effects of SAHA and RG7388 treatments on MCF-7 and LNCaP cells

Since the cell cycle related proteins offered interesting findings, we determined the apoptotic effects of SAHA and RG7388 treatments using the fluorescence staining method with DEVD-*amc* fluorogenic substrates that are specific for Caspase-3/7 (Figure 5A,6A). The fluorescence substrates DEVD was employed to mainly verify the activation of the caspases, particularly Caspase-3 and Caspase-7 following the drug treatments. As discussed above, the cells that were treated with RG7388

produced high levels of fluorescence in both MCF-7 and LNCaP, as a result of the cleavage of DEVD-*amc* substrate. Interestingly, SAHA treatment produced lower levels of fluorescence, possibly due to lesser cleavage of the substrate as a result of the lesser activation of apoptosis pathway. However, the light microscopic imaging of the unstained cells also showed significant reduction in the cell number after RG7388 treatment. The results of the imaging experiments were supported by the western blotting results of the PARP cleavage, BAX and BAK elevation that were performed after treating the cells with RG7388 (Figure 7,8). Interestingly, the SAHA treatment was not able to elevate BAX or BAK levels in MCF-7 and LNCaP cells, rather it produced a slight decrease after 24 hrs of treatment. In addition, SAHA treatment did not produce PARP cleavage, even after 24 hrs of treatment with 7.5 μM concentration (Figure 7,8). However, SAHA treatment showed measurable levels of cell death, but it was lower than the extend of cell death induced by RG7388 treatment after 24 hrs in both MCF-7 and LNCaP cells. So far, the greater effects of RG7388 is evidenced by the elevation of PARP cleavage that coincides well with increases in the levels of BAX and BAK, suggesting activation of the intrinsic pathway by this MDM2 inhibitor is leading to apoptotic cell death in the cancer cells.

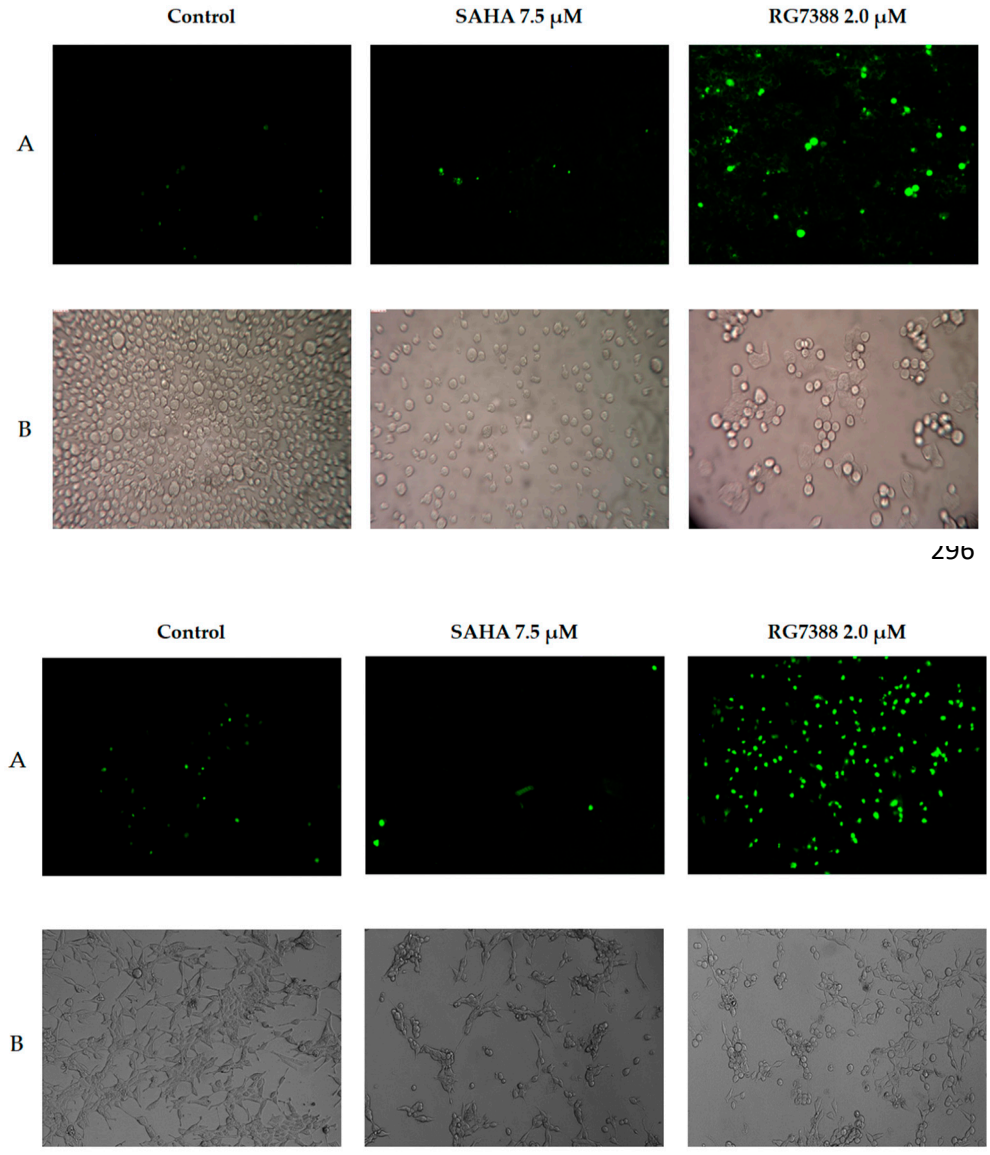

Figure 5 and 6. Apoptotic cell death in MCF-7 and LNCaP cells shown by Fluorescence image obtained using the DEVD-*amc*. The results of cell death induced by SAHA and RG7388 treatment for

Preprints (www.preprints.org) | NOT PEER-REVIEWED | Posted: 7 October 2018 doi:10.20944/preprints201810.0121.v1

Peer-reviewed version available at Medicina 2019, 55, 30; doi:10.3390/medicina55020030

312 24 hrs is shown in Figure 5A and 6A. The effects of the treatment on cell death observed in by light
313 microscopic imaging is shown in Figure 5B and 6B.

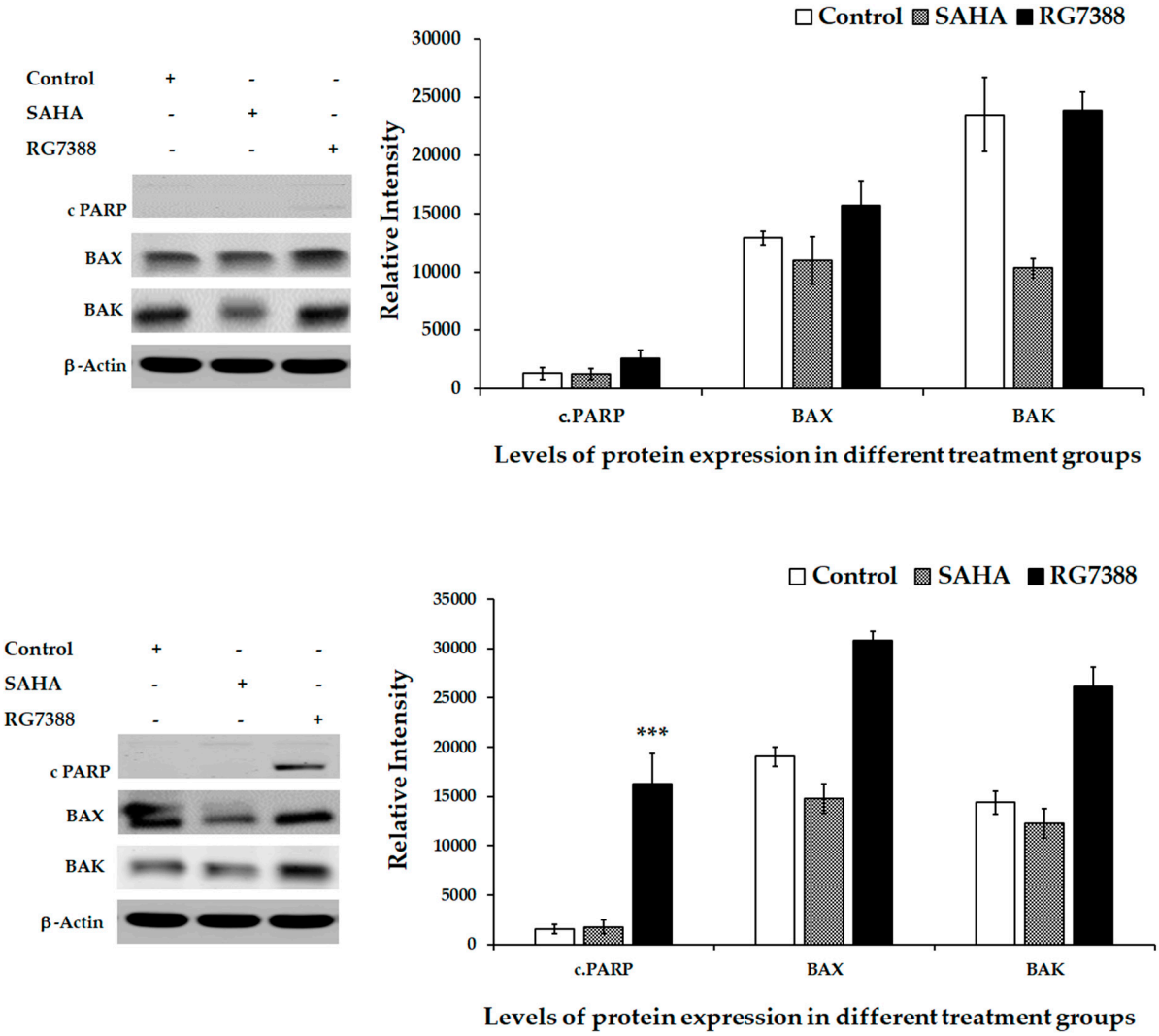

314 **Figure 7 and 8.** Apoptotic Markers detected by Western Blot. Figure shows the western blot analysis
315 of BAK, BAX and PARP (full length and cleaved PARP) expressions in treated on MCF-7 and LNCaP
316 cells. The density of the western blots bands shown in the right panel was quantified using ImageJ
317 software. Data are presented as means ± S.E.M. from minimum of three independent experiments.
318 The asterisk indicates that the comparison is statistically significant. *, $P < 0.05$ vs. Control; **, $P <$
319 0.001 vs. Control; ***, $P < 0.01$ vs. Control.

320 **4. Discussion**

321 Many studies so far have shown that DNA damage can lead to the up-regulation and
322 activation of p53 tumor suppressor protein, which can produce cell cycle arrest at the G to S transition
323 checkpoint, or leading to the induction of apoptosis through transcriptional activation of $p21^{WAF1/CIP1}$.
324 The $p27^{KIP1}$ protein that is encoded by the CDKN1B gene is also known to play a significant role in
325 inducing apoptosis. The $p27^{KIP1}$ belongs to the CIP/KIP family of CDKI proteins and is intimately

involved in regulating the progression of cells through the different phases of the cell cycle [26]. Both $p21^{WAF1/CIP1}$ and $p27^{KIP1}$ proteins can bind and prevent the activation of cyclin D, E, A and B-dependent kinases, in particular, block the activation of CDK2 by cyclin E or CDK4 by cyclin D, and thus controls the cell cycle progression from G1 to S phase [27,28]. Hence, both $p21^{WAF1/CIP1}$ and $p27^{KIP1}$ are commonly referred as cell cycle dependent kinase inhibitor (CDKI) proteins because of their ability to stop the cell division using CDK inhibitory mechanisms [27]. Many of the cell cycle arrest and anticancer effects of SAHA are known to be mediated through transcriptional induction of $p21^{WAF1/CIP1}$ gene and elevating its protein levels. It has been demonstrated that SAHA induced $p21^{WAF1/CIP1}$ promoter activity is primarily through two Sp1 sites located at 782 and 769 positions, relative to the transcription start site, in a p53-independent manner [29]. Though, Sp1 and Sp3 are the major transcription factors binding to the Sp1 site of the $p21^{WAF1/CIP1}$ promoter and induce gene expression, it was reported that SAHA did not alter their DNA binding activities. Since induction of $p21^{WAF1/CIP1}$ during SAHA treatment is mostly independent of p53, the acetylation-dependent mechanism is generally accounted for the observed induction of $p21^{WAF1/CIP1}$ expression in cells that lack functional p53. In addition, SAHA has been reported to induce hyperacetylation of the histones, which was shown to transcriptionally upregulate the expression of $p27^{KIP1}$ to cause co-inhibitory effects [30]. As result of the cell cycle arrest and apoptosis mediated death of cancer cells, regression of tumors in the *in vivo* models have been reported [31]. In further confirmation of the mechanistic ability of the CDKIs, the levels of $p27^{KIP1}$, were also found to be high in the quiescent cells that was found to decrease in the cancer cells, due to the sequestration into the cyclin D-CDK complexes. Therefore, the removal of $p27^{KIP1}$ mediated repression of CDK2 or CDK4 were reported to allow for the progression of cells through the G-S checkpoint more rapidly. The importance of $p27^{KIP1}$ in regulating the cell cycle was further confirmed by the fact that the mice that were null for the CDKN1B grew faster and exhibited organomegaly, and had higher incidence of pituitary tumors in comparison to age matched controls [32,33,34]. It has been previously reported that, overexpression of $p27^{KIP1}$ in cancer cells could result in strong G to S arrest and therefore it could be more cytotoxic to cancer cells relative to the effects of overexpression of $p21^{WAF1/CIP1}$ [35]. Similarly, through the study results that are presented here we are demonstrating the mechanism of $p21^{WAF1/CIP1}$ and $p27^{KIP1}$ induced cell cycle arrest and its possible role in inducing apoptosis during SAHA and RG7388 treatment.

So far, it has been well established that histone deacetylase inhibitors (HDACi), such as SAHA, can kill transformed cells or cancer cells that are in cultures or implanted in animal models [36]. Similarly, RG7388 has also produced cell cycle arrest and cell death through inhibition of the MDM2-p53 interaction and $p21^{WAF1/CIP1}$ elevation in our experiments. It is fully evident that RG7388 effects are mediated through p53 because, the X-ray crystal structures of N-terminal of MDM2 that complexes with N-terminal of p53 has revealed that the binding site of p53 in MDM2 is formed by 14 residues: Leu^{54}, Leu^{57}, Ile^{61}, Met^{62}, Tyr^{67}, Gln^{72}, Val^{75}, Phe^{86}, Phe^{91}, Val^{93}, His^{96}, Ile^{99}, Tyr^{100}, and Ile^{101}. MDM2 has a deep hydrophobic cleft on which the p53 protein, after adopting a α-helical conformation, interacts primarily through three hydrophobic residues: Phe^{19}, Trp^{23} and Leu^{26} of p53, that are buried deeply in the MDM2 cleft. To disrupt this interaction MDM2 inhibitors must mimic primarily these three hydrophobic interactions. Molecular modelling and simulation studies have so far revealed that, 4-chlorophenyl and neopentyl group of RG7388 occupy the Trp^{23} and Phe^{19} pockets, while its 3-chlorophenyl group occupies the Leu^{26} pocket and participates in an additional π–π interaction with the His^{96} residue. In addition, the pyrrolidine Cα carbonyl was shown to form a

hydrogen bond with NH of His^{96} [25]. Although, RG7388 and some of the other MDM2 inhibitors such as Nutlin-3 have a shared mechanism of action, RG7388 has superior potency and specificity for MDM2 compared to the other MDM2 inhibitors. The greater potency of RG7388 is probably responsible for the stronger cell cycle arrest and the cell death effects observed. From our studies it is very clear that, in LNCaP prostate cancer cells SAHA and RG7388 were able to significantly induce cell cycle arrest, through elevation of $p21^{WAF1/CIP1}$ and $p27^{KIP1}$ that was leading to apoptosis (Figure 9B). In this process of executing the apoptotic cell death, elevation BAX and BAK leading to PARP cleavage appears to be intimately involved following the treatment of LNCaP cells with RG7388. However, in MCF-7 cells there was only $p27^{KIP1}$ elevation and there was no noticeable elevation of $p21^{WAF1/CIP1}$, BAX or BAK to induce apoptosis. This interesting observation suggested that the RG7388 induced cell death in the MCF-7 breast cancer cell line is probably executed by $p27^{KIP1}$, through mechanisms that does not require BAX or BAK elevation (Figure 9A). Another interesting observation from our experiments is the differential abilities of SAHA and RG7388 for inducing cell cycle arrest and cell death. Very interestingly, SAHA was able to elevate $p21^{WAF1/CIP1}$ expression without elevating the p53 levels in both MCF-7 and LNCaP cells. As expected, inhibition of MDM2 with RG7388 was able to induce $p21^{WAF1/CIP1}$ expression by re-activating p53 in LNCaP cells due to strong inhibition of MDM2 [37]. Several earlier studies have analyzed the status and role of cyclins D and E in growth-arrested prostate cancer cells and pointed to the distinct classes of genes that might be involved in the regulatory process of prostate cancer cell growth [38,39,40,41,42,43,44,45]. Another important master switch in the in cell cycle regulation is Rb, and its status of phosphorylation parallels cell transit through G1 into the S phase [46,47]. An important mechanism that regulates the Rb phosphorylation and controls the cell cycle progression is through cyclin D and the cdk4/6 complex. The activated cyclin D/CDK4 complex can phosphorylate Rb and prevent its inhibitory binding to E2F, facilitating the entry of cells from G1 into S phase [48]. It appears that the RG7388 treatment might be inhibiting CDK1 through blocking the AURKB pathway that involves CDC25C also. However, majority of the cell cycle arrest effects of $p21^{WAF1/CIP1}$ are believed to be mediated through inhibition of Rb phosphorylation. Hence, the role of Rb cannot be ruled out in mediating cell death caused by SAHA treatment. However, results of another study has demonstrated very clearly that drugs such as celecoxib could increase the expression of $p27^{KIP1}$ proteins and induce cell death. Interestingly, the study with celecoxib showed that the rate of apoptosis was higher with the activation of $p27^{KIP1}$. Based on that evidence it was suggested that the up-regulation of $p27^{KIP1}$ may contribute to the induction of cell cycle arrest and apoptosis even when $p21^{WAF1/CIP1}$ levels are not altered [49,50].

Preprints (www.preprints.org) | NOT PEER-REVIEWED | Posted: 7 October 2018 doi:10.20944/preprints201810.0121.v1

Peer-reviewed version available at Medicina 2019, 55, 30; doi:10.3390/medicina55020030

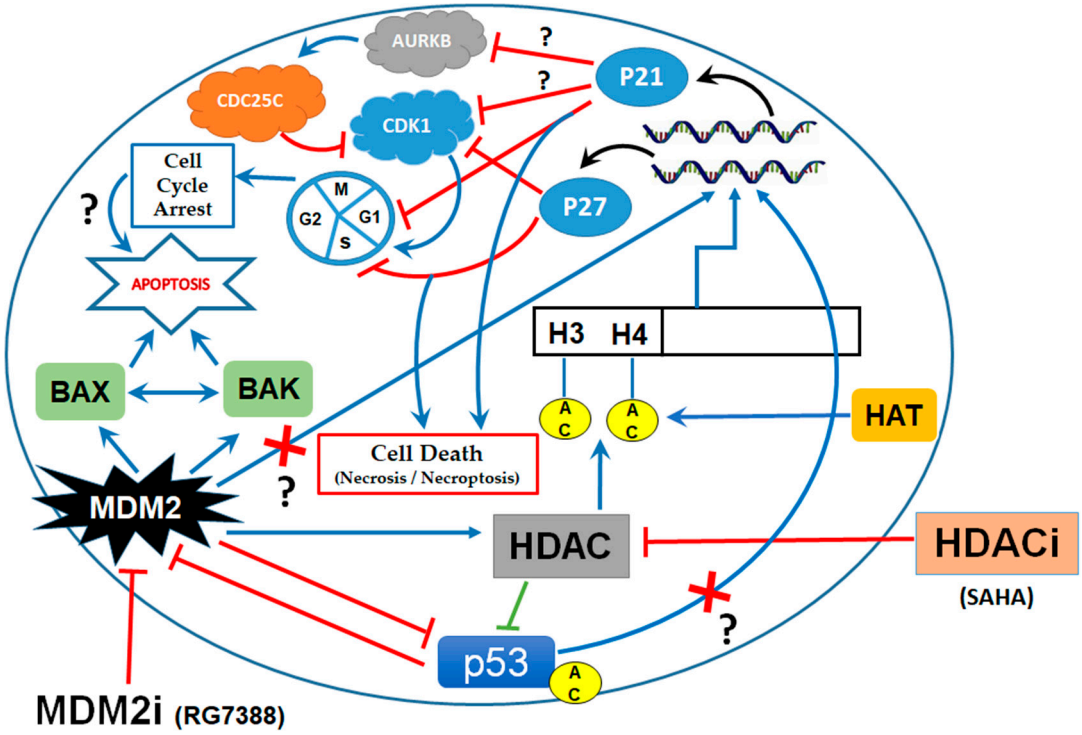

412

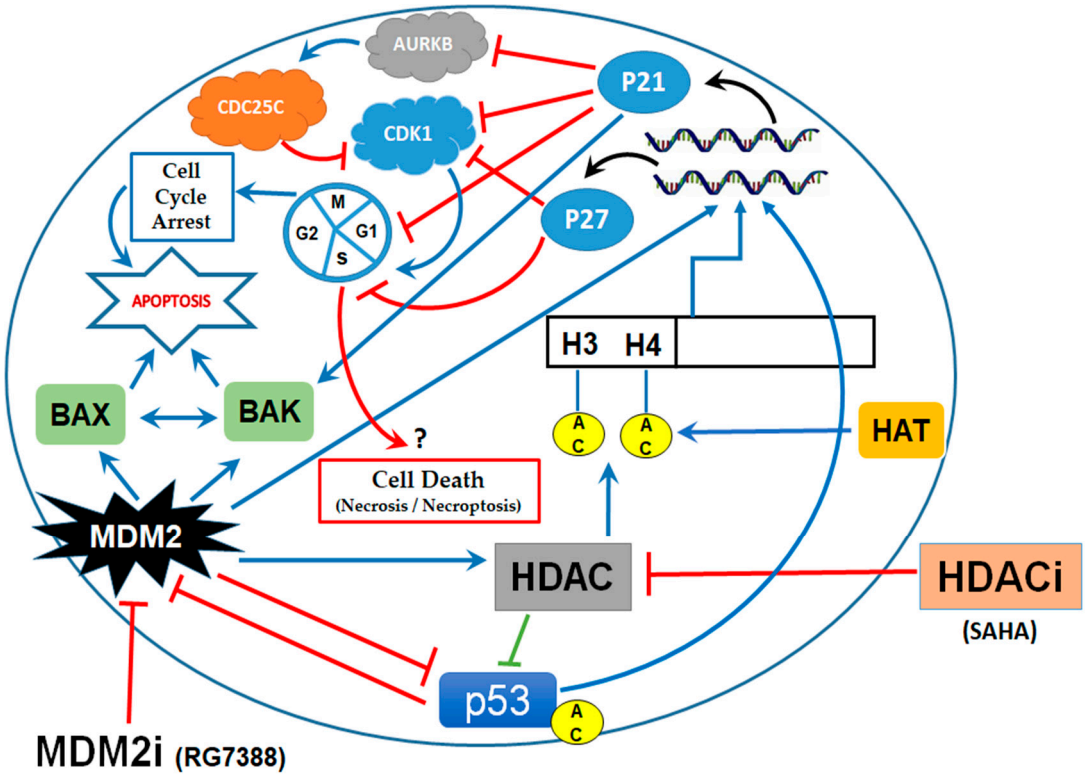

413

Figure 9A and 9B. Pathways Impacted by SAHA in LNCaP and MCF-7 Cells. The figure 9A illustrates the pathways activated by SAHA in MCF-7 cells leading to cell death. 9B illustrates the cycle arrest and the apoptosis pathway triggered by MDM2 inhibitor (RG7388) and HDACi (SAHA) in LNCaP cells.

5. Conclusions

Thus, our results suggest that the cell death caused by SAHA treatment in both cell lines was primarily through induction of $p21^{WAF1/CIP1}$ and $p27^{Kip1}$ levels, that is independent of p53. In support of this conclusion it has been reported in the literature that the elevated levels of acetylated histones (H2 and H3) and consequent activation of intracellular signals including $p21^{WAF1/CIP1}$ elevation are responsible for the cell cycle arrest and cell death that are typically observed in cancer cells when HDAC inhibitors (HDACi) are used. On the other hand, in our experiments the RG7388 treatment was able to induce cell death by elevating $p21^{WAF1/CIP1}$ through p53 dependent mechanism in LNCaP cells through inhibition of MDM2. Interestingly, the RG7388 treatment was not able to elevate $p21^{WAF1/CIP1}$ in MCF-7 cells, even though there is evidence of p53 reactivation as it can be seen with its elevation. Hence, we suspect there is some level of uncoupling of p53 mediated transcriptional induction of $p21^{WAF1/CIP1}$ in MCF-7 cells. Thus, two different drugs which have the ability to induce p21 expression exhibited distinct mechanisms of cell death through p53 dependent and independent mechanisms. As it points to an interesting intracellular interplay between two or more cell cycle related pathways, confirmation of the actual cell death mechanism induced by RG7388 in MCF-7 in cancer cells requires additional exploration.

Author Contributions: A.R., U.N., T.V., V.R. and S.S conceived and designed the research and analyzed the data. U.N. and T.V. performed all the experiments summarized in the manuscript. The manuscript was written by U.N., and T.V., and then reviewed by A.R. and V.R. The study was supervised by A.R.

Acknowledgments: This research was supported by the Royal Dames of Cancer Research Inc of Fort Lauderdale, Florida. For their financial support.

Conflicts of Interest: The authors declare that they have no conflict of interest.

References

1. Cheng, M.H.; Wong Y.H.; Chang C.M.; Yang, C.C.; Chen, S.H.; Yuan, C.L.; Kuo H.M.; Yang, C.Y.; Chiu, H.F. B1, a novel HDAC inhibitor, induces apoptosis through the regulation of STAT3 and NF-κB. *Int. J. Mol. Med.***2017,** 39, 1137-1148. doi: 10.3892/ijmm.2017.2946.
2. Somasundar, P.; Yu, A.K.; Vona-Davis, L.; McFadden, D.W. Differential effects of Leptin on cancer *in vitro*. *J. Surg. Res.***2003,** 113, 50-55.
3. Connolly, R.; Stearns, V. Epigenetics as a therapeutic target in breast cancer. *J. Mammary Gland Biol.Neoplasia.***2012,** 17, 191-204. DOI:10.1007/s10911-012-9263-3
4. Drummond, D.C.; Noble, C.O.; Kirpotin, D.B.; Guo, Z.; Scott, G.K.; Benz, C.C. Clinical development of histone deacetylase inhibitors as anticancer agents. *Annu. Rev. Pharmacol. Toxicol.***2005,** 45, 495–528. DOI:10.1146/annurev.pharmtox.45.120403.095825
5. De Ruijter, A.J.; Van Gennip, A.H.; Caron, H.N.; Kemp, S.; Van Kuilenburg, A.B. Histone deacetylases (HDACs): characterization of the classical HDAC family. *Biochem J.***2003,** 370, 737-749. DOI:10.1042/BJ20021321

6. Munster, P.N.; Troso-Sandoval, T.; Rosen, N.; Rifkind, R.; Marks, P.A.; Richon, V.M. The histone deacetylase inhibitor suberoylanilidehydroxamic acid induces differentiation of human breast cancer cells. *Cancer Res.***2001,** 61, 8492-8497.
7. Gregoretti, I.V.; Lee, Y.M. Goodson, H.V. Molecular evolution of the histone deacetylase family: functional implications of phylogenetic analysis. *J. Mol. Biol.***2004,** 338, 17-31. DOI: 10.1016/j.jmb.2004.02.006
8. Thiagalingam, S.; Cheng, K.H.; Lee, H.J.; Mineva, N.; Thiagalingam, A.; Ponte, J.F. Histone deacetylases: unique players in shaping the epigenetic histone code. *Ann. N. Y Acad. Sci.***2003,** 983, 84-100
9. Weiqiang, Z.; Xiuyan, F.; Han, H.; Shanchun, G., Guangdi, W. Synergistic effects of combined treatment with histone deacetylase inhibitor suberoylanilidehydroxamic acid and TRAIL on human breast cancer cells. *Sci. Rep.***2016,** 6, 28004. DOI: 10.1038/srep28004
10. Munster, P.N.; Thurn, K.T.; Thomas, S.; Raha, P.; Lacevic, M.; Miller, A.; Melisko, M.; Ismail-Khan, R., Rugo, H.; Moasser, M.; Minton, S.E. A phase II study of the histone deacetylase inhibitor vorinostat combined with tamoxifen for the treatment of patients with hormone therapy-resistant breast cancer. *Brit. J. Cancer.***2011,** 104, 1828-1835. DOI: 10.1038/bjc.2011.156
11. Lidia, C.S.; Denise, D.F.; Sonya, Z.; Paul, O.K.; Helena, C.; Nancy, T.; Hong, X.; Dalia, C. Histone Deacetylase Inhibition Selectively Alters the Activity and Expression of Cell Cycle Proteins Leading to Specific Chromatin Acetylation and Antiproliferative Effects. *J. Biol. Chem.***1999,** 274, 34940-34947. doi: 10.1074/jbc.274.49.34940
12. Rathinavelu, A.;Narasimhan, M.;Muthumani, P. A Novel Regulation of VEGF Expression by HIF-1α and STAT3 in HDM2 transfected Prostate Cancer Cells. *J. of cellular and Molecular Medicine*, **2011,**16.
13. Fakharzadeh, S. S.; Trusko, S. P.; George, D.L.Tumorigenic potential associated with enhanced expression of a gene that is amplified in a mouse tumor cell line.*EMBO J.*1991,10, 1565-1569.
14. Oliner, J. D.;Kinzler, K. W.; Meltzer, P. S.; George, D. L.; Vogelstein, B. Amplification of a gene encoding a p53-associated protein in human sarcomas.*Nature,***1992,**358, 80-83. DOI:10.1038/358080a0
15. Kussie, P.H.;Gorina, S.;Marechal, V.;Elenbaas, B.; Moreau, J.; Levine, A. J.;Pavletich, N.P. Structure of the MDM2 oncoprotein bound to the p53 tumor suppressor transactivation domain.*Science,*1996,274, 948-953.
16. Hu, B.; Gilkes, D.M.; Farooqi, B.; Sebti, S.M.; Chen, J. MDMX overexpression prevents p53 activation by the MDM2 inhibitor Nutlin.*J. Biol. Chem.* ***2006,***281, 33030-33035.DOI:10.1074/jbc.C600147200
17. Sigalas, I.; Calvert, A.H.; Anderson, J.J.; Neal, D.E.; Lunec, J. Alternatively spliced mdm2 transcripts with loss of p53 binding domain sequences: transforming ability and frequent detection in human cancer.*Nat. Med.***1996,**2, 912-917.
18. Jones, S. N., Hancock, A. R., Vogel, H., Donehower, L. A., and Bradley, A. Overexpression of Mdm2 in mice reveals a p53-independent role for Mdm2 in tumorigenesis*Proc. Natl. Acad. Sci. U. S. A.* **1998,**95, 15608-15612.

19. Bartel, F.;Pinkert, D.; Fiedler, W.;Kappler, M.; Wurl, P.; Schmidt, H.;Taubert, H. Expression of alternative and aberrantly spliced transcripts of the MDM2 mRNA is not tumor-specific. *Int. J. Oncol*. **2004,**24, 143-151.https://doi.org/10.3892/ijo.24.1.143
20. Ramakrishnan, R.; Zell, J.A.; Malave, A.; Rathinavelu, A. Expression of Vascular Endothelial Growth Factor mRNA in GI-101A and HL-60 Cell Lines. *Bioche. Biophys. Res. Commun*. 2000, 270, 709-713. https://doi.org/10.1006/bbrc.2000.2493
21. Narasimhan, M.; Rose, R.; Karthikeyan, M.; Rathinavelu, A. Detection of HDM2 and VEGF co-expression in cancer cell lines: novel effect of HDM2 antisense treatment on VEGF expression. *Life Sci*. 2007, 81, 1362 1372. https://doi.org/10.1016/j.lfs.2007.08.029
22. Vassilev ,L.T.; Vu, B.T.; Graves, B.; Carvajal, D.; Podlaski, F.; Filipovic, Z.; Kong, N.; Kammlott, U.; Lukacs, C.; Klein, C.; Fotouhi, N. et al . In vivo activation of the p53 pathway by small-molecule antagonists of MDM2. *Science*. **2004,** 303, 844–48. DOI:10.1126/science.1092472
23. Lakoma, A.; Barbieri, E.; Agarwal, S.; Jackson, J.; Chen, Z.; Kim, Y.; McVay, M.; Shohet, J.M.; Kim, E.S. The MDM2 small-molecule inhibitor RG7388 leads to potent tumor inhibition in p53 wild-type neuroblastoma. *Cell Death Discov.* 2015, Article number: 15026. https://doi.org/10.1038/cddiscovery.2015.26
24. Vu, B.T.; Vassilev, L. Small-molecule inhibitors of the p53-MDM2 interaction. *Curr. Top. Microbiol. Immunol.* **2011,** 348, 151-172. DOI:10.1007/82_2010_110
25. Ding, Q.; Zhang, Z.; Liu, J.J.; Jiang, N.; Zhang, J.; Ross, T.M.; Chu, X.J.; Bartkovitz, D.; Podlaski, F.; Janson, C. et al. Discovery of RG7388, a potent and selective p53-MDM2 inhibitor in clinical development. *J. Med. Chem.* **2013,** 56, 5979-5983. DOI:10.1021/jm400487c
26. Katayose, Y.; Kim, M.; Rakkar, A.N.; Li, Z.; Cowan, K.H.; Seth, P. Promoting apoptosis: a novel activity associated with the cyclin-dependent kinase inhibitor p27. *Cancer Res.* **1997,** 57: 5441–5445.
27. Sherr, C.J.; Cancer cell cycles. *Science*. **1996,** 274, 1672-1677.
28. Polyak, K.; Lee, M.H.; Erdjument-Bromage, H.; Koff, A.; Roberts, J.M.; Tempst, P.; Massagu, Ã.J. Cloning of p27Klpl, a cyclin-dependent kinase inhibitor and a potential mediator of extracellular antimitogenic signals. *Cell*. **1994,** 78, 59-66.
29. Lili, H.; Yoshihiro, S.; Toshiyuki, S.; Arthur, B.P. () Activation of the p21WAF1/CIP1 promoter independent of p53 by the histone deacetylase inhibitor suberoylanilidehydroxamic acid (SAHA) through the Sp1 sites. *Oncogene.* **2000,** 19, 5712-5719. DOI:10.1038/sj.onc.1203963
30. Purva, B.; Michael, P.; Ramona, S.; Warren, F.; Hirohito, Y.; Maria, B.; Kathy, R.; Hong-Gang, Wang.; Victoria, R.; Kapil, B. Activity of SuberoylanilideHydroxamic Acid Against Human Breast Cancer Cells with Amplification of Her-2. *Clin. Cancer Res.* **2005,** 11, pp 6382. DOI: 10.1158/1078-0432.CCR-05-0344
31. Cohen, L.A.; Marks, P.A.; Rifkind, R.A.; Amin, S.; Desai, D.; Pittman, B.; Richon, V.M. .et al. Suberoylanilidehydroxamic acid (SAHA), a histone deacetylase inhibitor, suppresses the growth of carcinogen induced mammary tumors. *Anticancer Res.* **2002,** 22, 1497-1504.
32. Nakayama, K.; Ishida, N.; Shirane, M.; Inomata, A.; Inoue, T.; Shishido, N.; Horii, I.; Loh, D.Y.; Nakayama, K. Mice lacking p27(Kipl) display increased body size, multiple organ hyperplasia, retinal dysplasia, and pituitary tumors. *Cell.* **1996,** 85, 707-720.

33. Fero, M.L.; Rivkin, M.; Tasch, M.; Porter, P.; Carow, C.E.; Firpo, E.; Polyak, K.; Tsai, L.H.; Broudy, V.; Perlmutter, R.M.; Kaushansky, K.; Roberts, J.M. A syndrome of multiorgan hyperplasia with features of gigantism, tumorigenesis, and female sterility in p27(Kipl)-deficient mice. *Cell*, 85, 733-744, 1996.
34. Kiyokawa, H.; Kineman, R.D.; Manova-Todorova, K.O.; Scares, V.C.; Hoffman, E.S.; Ono, M.; Khanam, D.; Mayday, A.C.; Frohman, L.A.; Koff, A. Enhanced growth of mice lacking the cyclin-dependent kinase inhibitor function of p27(Kipl). *Cell.* **1996,** 85, 721-732.
35. Craig, C.; Wersto, R.; Kim, M.; Ohri, E.; Li, Z.; Katayose, D.; Lee, S.J.; Trepel, J.; Cowan, K.; Seth, P. A recombinant adenovirus expressing p27Kipl induces cell cycle arrest and loss of cyclin-Cdk activity in human breast cancer cells. *Oncogene.* **1997,** 14, 2283-2289.
36. Paul, A.M.; Victoria, M.R.; Thomas, M.; William, K.K. Histone Deacetylase Inhibitors. *Adv. in Cancer Res.* **2004,** 137-168.
37. Umamaheswari, N.; Thiagarajan, V.; Vijayaraghavan, R.; Shila, S.; Rathinavelu, A. Comparative Effects of HDAC Inhibitor SAHA and MDM2 Inhibitor RG7388 in LNCaP Prostate Cancer Cells. **2018,** 8. 10.26717/BJSTR.2018.08.001677
38. Schwarze, S.R.; Shi, Y.; Fu, V. X.; Watson, P.A.; Jarrard, D.F. Role of cyclin-dependent kinase inhibitors in the growth arrest at senescence in human prostate epithelial and uroepithelial cells. *Oncogene.* **2001,** 20, 8184–8192. DOI:10.1038/sj.onc.1205049
39. Milanesa, D.M.; Choudhury, M.S.; Mallouh, C.; Tazaki, H.; Konno, S. Methylglyoxal-induced apoptosis in human prostate carcinoma: potential modality for prostate cancer treatment. *Eur. Urol.* **2000,** 37: 728-734. DOI:10.1159/000020226
40. Tsihlias, J.; Zhang, W.; Bhattacharya, N.; Flanagan, M.; Klotz, L.; Slingerland, J. Involvement of p27Kip1 in G1 arrest by high dose 5-dihydrotestosterone in LNCaP human prostate cancer cells. *Oncogene.* **2000,** 19, 670-679. **DOI:** 10.1038/sj.onc.1203369
41. Singh, G.; Lakkis, C.L.; Laucirica, R.; Epner, D.E. Regulation of prostate cancer cell division by glucose. *J. Cell. Physiol.* **1999,** 180, 431-438.
42. Aaltomaa, S.; Eskelinen, M.; Lipponen, P. Expression of cyclin A and D proteins in prostate cancer and their relation to clinicopathological variables and patient survival. *Prostate.* **1999,** 38, 175-182.
43. Guinan, P.; Shaw, M.; Mirochnik, Y.; Slobodskoy, L.; Ray, V.; Rubenstein, M. Paclitaxel is more effective than thalidomide in inhibiting LNCaP tumor growth in a prostate cancer model. Methods Findings. *Exp. Clin. Pharmacol.* **1998,** 20, 739-742.
44. Perry, J.E.; Grossmann, M.E.; Tindall, D. J. Epidermal growth factor induces cyclin D1 in a human prostate cancer cell line. *Prostate.* **1998,** 35, 117-124.
45. Itoh, N.; Kakehi, Y.; Akao, T.; Kinoshita, H.; Okada, Y.; Yoshida, O. Concomitant presence of p16/cyclin-dependent kinase 4 and cyclin D/cyclin-dependent kinase 4 complexes in LNCaP prostatic cancer cell line. *Jpn. J. Cancer Res.* **1997,** 88, 229-233.
46. Weinberg, R.A. The retinoblastoma protein and cell cycle control. *Cell.* **1995,** 81, 323-330.
47. Bartek, J.; Bartkova, J.; Lukas, J. The retinoblastoma protein pathway and the restriction point. Curr. *Opin. Cell Biol.* **1996,** 8, 805-814.
48. Kato, J.; Matsushime, H.; Heibert, S.W.; Ewen, M.E.; Sherr, C.J. Direct binding of cyclin D to the retinoblastoma gene product(pRb) and pRb phosphorylation by the cyclin D-dependent kinase CDK4. *Genes Dev.* **1993,** 7, 331-342.

585 49. Katayose, Y.; Kim, M.; Rakkar, A.N.; Li, Z.; Cowan, K.H.; Seth, P. Promoting apoptosis: a
586 novel activity associated with the cyclin-dependent kinase inhibitor p27. Cancer Res. **1997,**
587 57, 5441-5445.
588 50. Furuya, Y.; Akimoto, S.; Yasuda, K.; Ito, H. Apoptosis of androgen-independent prostate cell
589 line induced by inhibition of fatty acid synthesis. Anticancer Res. 1997, 17, 4589-4593.